

Petedunnite (CaZnSi₂O₆), a new zinc clinopyroxene from Franklin, New Jersey, and phase equilibria for zincian pyroxenes*

ERIC J. ESSENE, DONALD R. PEACOR

Department of Geological Sciences, University of Michigan, Ann Arbor, Michigan 48109, U.S.A.

ABSTRACT

A zinc clinopyroxene with the formula



has been found in the zinc deposit in Franklin, New Jersey. Because Zn is the dominant M1 cation, this phase is a new mineral species, and the endmember is considered to be CaZnSi₂O₆. It has been named for Dr. Pete J. Dunn of the Smithsonian Institution in recognition of his extensive work on Franklin minerals. The X-ray, chemical, and optical data are consistent with the interpretation of petedunnite as a clinopyroxene with space group *C2/c*. Unit-cell parameters are $a = 9.82(3)$, $b = 9.00(1)$, $c = 5.27(2)$ Å, $\beta = 105.6(2)^\circ$, $V = 448(2)$ Å³. Plots of available chemical analyses suggest extensive solid solution between petedunnite and diopside-hedenbergite-johannsenite. Petedunnite is dark green, has a calculated density of 3.68 g/cm³ and has {110} cleavages. Optical properties are $\alpha = 1.68(1)$, $\beta = 1.69(1)$, $\gamma = 1.70(1)$, $2V_z = 80(5)^\circ$, $Z \wedge c = 40(5)^\circ$, $Y \parallel b$, $X, Y = \text{light yellow}$, $Z = \text{light green}$, $r > v$ (strong).

Preliminary high-pressure experiments at 20 kbar and 900°C have yielded the phase CaZnSi₂O₆, with $a = 9.803(6)$, $b = 8.975(7)$, $c = 5.243(7)$ Å, $\beta = 105.75(7)^\circ$, $V = 444.0(9)$ Å³, $\rho_{\text{calc}} = 3.853(8)$ g/cm³. The lower-pressure assemblage hardystonite (Ca₂ZnSi₂O₇) + willemite (Zn₂SiO₄) + quartz will buffer the CaZnSi₂O₆ content of a coexisting clinopyroxene solid-solution at a maximum for given *P-T* conditions. Petedunnite substitution is also buffered in clinopyroxene solid-solution as a function of the ratio $f_{\text{O}_2}/f_{\text{S}_2}$ in the presence of wollastonite + sphalerite + quartz. Phase equilibria calculated from thermodynamic data collated for phases in the system Zn-Al-Si-O-S suggest that much of the Franklin area zinc ore formed at a relatively high fugacity ratio of $f_{\text{O}_2}/f_{\text{S}_2}$ that was presumably inherited from a S-poor premetamorphic protore.

INTRODUCTION

Dr. Pete J. Dunn sent us a rather unusual-appearing hand specimen collected at Franklin, New Jersey, which he had tentatively identified as a Zn-rich clinopyroxene. Preliminary microprobe analysis suggested that the Zn content of the pyroxene is sufficiently high to define this material as a new mineral species. Although zincian clinopyroxenes (varieties jeffersonite and zinc-schefferite: Palache, 1935) are not unusual at Franklin and Sterling Hill, they are all rich in Mg and/or Mn and do not have Zn as the dominant M1 cation. We therefore carried out detailed studies of the Zn-rich pyroxene and confirmed that some portions of the specimen contain sufficient Zn in the M1 site to warrant species status. We have named this mineral *petedunnite* in honor of Dr. Pete J. Dunn of the Department of Mineral Sciences, Smithsonian Institution, Washington, D.C., in recognition of his many contributions to mineralogy, especially at Franklin and

Sterling Hill, New Jersey. The name and mineral status have been approved by the IMA Commission on New Minerals and Mineral Names. The holotype specimen of petedunnite is in the collection of the Smithsonian Institution with catalogue number NMNH 162211, and fragments preserved during this study for preparation of thin sections and single-crystal mounts are stored in the Mineralogical Collections, Department of Geological Sciences, University of Michigan.

OCCURRENCE

Petedunnite is known in a single unusual hand specimen from Franklin, New Jersey. The specimen is approximately 10 cm in diameter and consists largely of dark green, anhedral clinopyroxene surrounded by light green clinopyroxene and massive calcite. Although the pyroxene appears to be a homogeneous single crystal in hand specimen, in thin section it is seen to be a mosaic of 10–100- μm -sized, parallel to subparallel clinopyroxene subgrains containing inclusions of isotropic and anisotropic minerals with grain sizes on the order of 1–10 μm .

* Contribution no. 408 from the Mineralogical Laboratory, Department of Geological Sciences, University of Michigan.

Table 1. Mineral inclusions in petedunnite

Mineral	Chemistry*	Abundance	Luminescence**	Optical observation
Willemite	Zn, Si	common	brilliant green	scattered blebs and veins
Calcite	Ca, (Mn)	common	brilliant red	colorless
Genthelvite	Si, Zn, S	common	brilliant blue	isotropic, colorless
Garnet	Si, Ca, Fe, Al	common	none	isotropic, yellow
Gahnite	Al, Zn	common	blue	isotropic, faint green
Albite	Si, Al, Na	common	light blue	anisotropic, colorless
Quartz	Si	uncommon	faint violet	anisotropic, colorless
Galena	Pb, S	uncommon	none	opaque blebs
Sphalerite	Zn, S	rare	brilliant blue	micrometer-sized specks
Sphene	Ca, Ti, Si	rare	none	not found
Apatite	Ca, As, P	rare	none	not found
Allanite	Si, Al, Ca, Ce	rare	none	not found
Iron oxide	Fe, (Mn)	rare	none	veining garnet
Unidentified	Si, Zn, Na?†	rare	blue	not found
Unidentified‡	Si, Al, Ca, (Mn)	rare	pinkish orange	not found

* Listed in order of decreasing weight fraction for elements with $Z > 10$ as determined by EDA; parentheses mark minor elements (<1 wt%).

** As observed at 15 kV and 0.3 a beam current; similar luminescent colors were observed in the luminescope at 10–15 kV.

† The presence or absence of Na cannot be resolved by EDA in the presence of major Zn.

‡ Possibly a zeolite.

Mineral identifications were made with qualitative energy-dispersive analytical X-ray data obtained on the University of Michigan ARL-EMX microprobe, supplemented by optical and luminescopic observations. Mineral inclusions in the pyroxene were identified as shown in Table 1. Fifteen different phases were identified, including eight luminescent minerals and three transparent, isotropic minerals. It is difficult to confirm equilibrium phase assemblages in this sample, but the genthelvite is closely associated with gahnite in a manner suggesting an equilibrium relationship.

The clinopyroxene is variable in composition with replacement of Zn by Mg and Mn. The areas with dominant Zn (petedunnite) may have formed by exchange of original diopside-hedenbergite-johannsenite solid solutions with the Zn-rich fluids that also caused precipitation of willemite, gahnite, genthelvite, and sphalerite. Because of the variable chemistry of the clinopyroxene, it was necessary to obtain analytical, optical, and X-ray data on only those portions of pyroxene with the highest Zn concentrations as established in thin section by prior electron-microprobe analysis.

X-RAY CRYSTALLOGRAPHY

Weissenberg and precession photographs were obtained on a cleavage fragment of Zn-rich clinopyroxene separated from a polished thin section. The photographs have extinctions and symmetry consistent with space groups $C2/c$ and Cc ; the former is assumed to be the true space group by analogy with other clinopyroxenes. The lattice parameters of natural petedunnite were refined by least squares using powder data obtained with a polycrystalline sample with a 114.6-mm-diameter Gandolfi camera and $CuK\alpha$ radiation with Si as internal standard. The lattice parameters of synthetic $CaZnSi_2O_6$ were refined from data collected on an X-ray powder diffractometer with a graphite monochromator using $CuK\alpha$ radi-

ation and fluorite as an internal standard. The powder data are listed in Table 2, and the refined lattice parameters from uniquely indexed reflections are given in Table 3. Ribbe and Prunier (1977) showed how the parameters a , b , and $c \sin \beta$ vary as a function of the radii of the M1 and M2 cations in pyroxenes of space group $C2/c$. Using their regression equations and assuming the site occupancies given below, we calculate values $a = 9.82$, $b = 8.99$, and $c \sin \beta = 5.09 \text{ \AA}$ for natural petedunnite. These are very similar to the observed values (Table 3) and support the occupancies inferred from the electron-microprobe analyses.

CHEMISTRY

Natural petedunnite was analyzed by Dr. P. J. Dunn with an ARL-SEM-Q electron microprobe using an operating voltage of 15 kV and a sample current of $0.025 \mu\text{a}$. Standards were Kakanui hornblende (Si, Ca, Mg, Al, Fe, Na), manganite (Mn), and synthetic ZnO (Zn). Data were corrected using the procedures of Bence and Albee (1968) and are given in Table 4. The derived formula, when normalized to four cations and six oxygens, is $(Ca_{0.92}Na_{0.06}Mn_{0.02})(Zn_{0.37}Mn_{0.18}Mg_{0.14}Fe_{0.19}^{2+}Fe_{0.12}^{3+})(Si_{1.94}Al_{0.06})O_6$. This formula and the X-ray observations are consistent with a diopside-like structure having an eight-fold-coordinated M2 site (largely occupied by Ca), and an octahedrally coordinated M1 site (with Zn as the dominant cation). Assigning of some of the Fe into the ferric state provides a charge balance for Na in the M2 site and Al in the tetrahedral site. The ideal end-member composition for petedunnite is $CaZnSi_2O_6$.

The petedunnite analysis is compared to the analyses of zincian diopside (variety jeffersonite) of Palache (1935) in Table 4. Petedunnite is lower in Mn + Mg and higher in Zn than these diopsides. The analyses in Palache appear somewhat questionable as they have poor totals (for wet-chemical analyses), low Si (in the first analysis) and low

Table 2. X-ray powder-diffraction data for natural and synthetic petedunnite

Natural petedunnite			Synthetic CaZnSi ₂ O ₆			
<i>hkl</i>	<i>d</i> _{obs}	<i>d</i> _{calc}	<i>hkl</i>	<i>d</i> _{calc}	<i>d</i> _{obs}	<i>hkl</i>
10	6.49	6.52	110	6.50	6.52	40
5	4.76	4.73	200	4.72	4.72	18
2	4.50	4.50	020	4.49	4.48	9
—	—	4.42	11 $\bar{1}$	4.41	4.40	3
1	3.36	3.36	021	3.35	3.34	2
2	3.25	3.26	220	3.25	3.25	10
100	3.02	3.01	22 $\bar{1}$	3.001	3.001	100
40	2.96	2.95	310	2.968	2.966	45
2	2.906	2.909	31 $\bar{1}$	2.904	2.904	7
30	2.589	2.583	13 $\bar{1}$	2.575	2.573	40
—	—	2.537	221	2.526	—	—
80	2.537	2.536	20 $\bar{2}$	2.529	2.525b	90
—	—	2.536	002	2.523	—	—
—	—	2.364	400	2.359	2.357	3
1	2.324	2.322	311	2.315	2.313	4
10	2.227	2.229	31 $\bar{2}$	2.224	2.217	13
—	—	2.228	112	2.217	—	—
—	—	2.208	22 $\bar{2}$	2.199	2.202	2
—	—	2.172	330	2.168	2.167	6
10	2.137	2.147	33 $\bar{1}$	2.142	2.141	20
—	—	2.123	42 $\bar{1}$	2.117	2.116	13
2	2.060	2.057	041	2.050	2.049	3
30	2.022	2.022	40 $\bar{2}$	2.018	2.019	9
—	—	2.018	202	2.010	2.011	9
2	1.979	1.979	13 $\bar{2}$	1.972	1.971	2
—	—	—	—	1.958	—	2
5	1.910	—	—	1.907	—	1
10	1.874	—	—	1.869	—	6
—	—	—	—	1.788	—	2
10	1.770	—	—	1.764	—	14
—	—	—	—	1.719	—	1
—	—	—	—	1.679	—	3
—	—	—	—	1.661	—	1
—	—	—	—	1.632	—	10
—	—	—	—	1.625	—	15
—	—	—	—	1.573	—	3
—	—	—	—	1.559	—	5
—	—	—	—	1.535	—	6
—	—	—	—	1.530	—	5
—	—	—	—	1.506	—	6
—	—	—	—	1.495	—	6
—	—	—	—	1.450	—	1
—	—	—	—	1.430	—	8
—	—	—	—	1.414	—	6
—	—	—	—	1.413	—	4

Note: For natural petedunnite, intensities are visually estimated using CuK α , Ni-filtered radiation, Gandolfi camera with *D* = 114.6 mm, and Si as internal standard. For synthetic CaZnSi₂O₆, CuK α radiation; powder X-ray diffractometer with graphite monochromator; fluorite as internal standard.

Ca (in the second analysis). Nevertheless, there are clear affinities between zincian diopside and petedunnite.

The petedunnite analysis is plotted in the composition space CaZnSi₂O₆-CaMnSi₂O₆-Ca(Mg,Fe)Si₂O₆ and compared with other analyses available for zincian pyroxenes (Fig. 1). Data from the literature indicate that solid solution is extensive among diopside, hedenbergite, and johannsenite. Few clinopyroxenes have been analyzed for Zn. Smith (1966) reported levels of 0.01–0.09 wt% ZnO for analyses of 17 diopside-hedenbergite solid solutions. Burton et al. (1982) have given analyses of 30 hedenbergites with 0.03–0.21 wt% ZnO. However, pyroxenes from

Table 3. Refined unit-cell parameters for natural petedunnite and synthetic CaZnSi₂O₆

	Natural petedunnite	Synthetic CaZnSi ₂ O ₆
<i>a</i> (Å)	9.82(2)	9.803(6)
<i>b</i> (Å)	9.00(1)	8.975(7)
<i>c</i> (Å)	5.27(2)	5.243(7)
β (°)	105.6(2)	105.75(7)
<i>c</i> sin β (Å)	5.08(3)	5.046(8)
<i>V</i> (Å ³)	448.(2)	440.0(9)

the Franklin–Sterling Hill area may contain more significant solid solution of CaZnSi₂O₆ (Palache, 1935; Frondel and Ito, 1966; P. Dunn, written comm., 1984). Although there appears to be complete solid solution between natural impure petedunnite and diopside-hedenbergite-johannsenite, there is no indication of solid solution extending to ideal CaZnSi₂O₆ in natural parageneses.

PHYSICAL PROPERTIES

In hand specimen, petedunnite is dark green in color and translucent. Its hardness and density could not be accurately measured because of the abundance of foreign inclusions. A density of 3.68 g/cm³ was calculated from the unit-cell volume and the chemical analysis of natural petedunnite. Petedunnite exhibits {110} cleavages and has a vitreous luster. It does not luminesce either in short- or long-wavelength ultraviolet radiation or under the electron-microprobe beam at 15-kV operating voltage.

The optical properties of petedunnite are difficult to measure owing to the turbid nature of the sample and its strong dispersion. Attempts were made to measure the refractive index of the petedunnite crystal that was mounted for single-crystal study on a fiber using a spindle stage. However, this yielded poor results owing to the turbid nature of the crystal and its tabular shape. Approximate

Table 4. Chemical analysis for petedunnite compared with zincian diopsides from Franklin

	Petedunnite (this study)	Jeffersonite (Palache, 1935)	
SiO ₂	48.4	45.95	49.03
Al ₂ O ₃	1.2	0.85	0.86
Fe ₂ O ₃ *	3.8	9.47	0.00
FeO*	5.7	0.38	7.75
MnO	5.8	10.20	7.91
MgO	2.4	3.61	5.81
CaO	21.3	21.55	19.88
ZnO	12.6	10.15	7.14
Na ₂ O	0.7	—	—
Sum	101.9	102.16	98.38
Si	1.944	1.865	1.992
Al	0.057	0.040	0.041
Fe ³⁺	0.116	0.288	0.000
Fe ²⁺	0.190	0.013	0.263
Mg	0.144	0.217	0.352
Zn	0.374	0.303	0.214
Mn	0.197	0.349	0.272
Ca	0.917	0.933	0.865
Na	0.061	—	—

* Mole fractions of Fe²⁺ and Fe³⁺ and equivalent wt% FeO and Fe₂O₃ calculated to yield six oxygens when normalized to four cations.

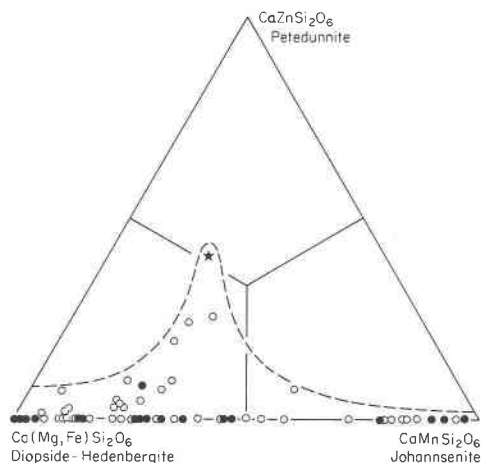


Fig. 1. Compositions of natural clinopyroxenes plotted in the space $\text{CaZnSi}_2\text{O}_6$ - $\text{CaMnSi}_2\text{O}_6$ - $\text{Ca}(\text{Mg,Fe})\text{Si}_2\text{O}_6$. Only pyroxenes with <4 wt% Al_2O_3 , Fe_2O_3 , or Na_2O are plotted. All zinciferous pyroxenes are from the Franklin area (Palache, 1935; Frondel and Ito, 1966; Dunn, written comm., 1984). Pyroxenes with $\text{Fe} > \text{Mg}$ are shown as solid circles, and those with $\text{Fe} < \text{Mg}$ as open circles. The type petedunnite (Table 4) is the starred point. The dashed line shows the observed limit of natural pyroxene solid solutions in this system.

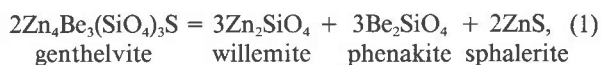
refractive indices, measured on cleavage fragments from the same area on the thin section as was used for single-crystal studies, using white light, a gelatin slide, and Cargille refractive index oils, are $\alpha = 1.68(1)$, $\beta = 1.69(1)$, $\gamma = 1.70(1)$. The optical angle, sign, and orientations, measured using a universal stage with 1.65 R.I. hemispheres and making no correction for tilts, are $2V_z = 80(10)^\circ$, $Z \wedge c = 40(5)^\circ$, $Y \parallel b$, $r > v$ (strong). These measurements are approximate owing to the strong dispersion of X , Z , and both optic axes in the (010) plane. Considering the relatively large errors in the measured refractive indices and optic axial angles, the two sets of optical data are considered to be in agreement. Flat-stage observations reveal weak pleochroism with X , $Y =$ light yellow, $Z =$ light green, $X = Y < Z$. These data may be compared with preliminary data on synthetic $\text{CaZnSi}_2\text{O}_6$, which has $\beta = 1.72(1)$, $Z \wedge c$ is large, and no pleochroism and dispersion were observed.

PETROLOGY

The mineral petedunnite may well be unique to the Franklin area as clinopyroxenes examined so far from other areas contain little or no Zn (Fig. 1). Even at Franklin Furnace, petedunnite is likely to be very rare because most clinopyroxenes have Zn subordinate to Mg (Fig. 1). Other Franklin pyroxenes coexisting with hardystonite and/or willemite + quartz should be analyzed to evaluate Zn-Mg exchange among pyroxene, melilite, and willemite. In addition, other Zn deposits such as Långban, Sweden, or Broken Hill, Australia, may eventually yield pyroxenes with significant contents of petedunnite component because of locally similar chemical environments. At Lång-

ban, an assemblage containing willemite + franklinite + awaruite (Nysten, 1984) requires low f_{S_2} to stabilize awaruite and willemite and relatively high f_{O_2} to allow significant Mn^{3+} in the franklinite. These conditions are similar to those of the Franklin area (see below). At Broken Hill, V. J. Wall and coworkers of Monash University have found ilmenite rich in ZnTiO_3 , which requires low- f_{S_2} conditions similar to those stabilizing zincite and willemite at Franklin (Wall, pers. comm., 1978). Zincian clinopyroxenes should also be sought in these and related assemblages to further evaluate the importance of petedunnite solid solutions.

The find of genthelvite at Franklin is of interest, first because it is a newly reported mineral for this area (Palache, 1935; Frondel, 1972; P. J. Dunn, written comm., 1983). Its presence in the petedunnite-bearing rock also suggests that the willemite in the rock could have significant solid solution of Be_2SiO_4 , or that phenakite (Be_2SiO_4 , willemite structure) could also occur at Franklin. Experiments on the Zn_2SiO_4 - Be_2SiO_4 join (Hahn and Eysel, 1970; Chatterjee and Ganguli, 1975) show that ~20–30 mol% Be_2SiO_4 may substitute into Zn_2SiO_4 coexisting with nearly pure Be_2SiO_4 at high T (1200–1300°C). Although the maximum solid solution of Be_2SiO_4 in Zn_2SiO_4 will decrease with decreasing T , several mole percent may possibly still persist in willemite that formed at moderate T (700–800°C). The reaction



which may govern a stability limit of genthelvite, also suggests that activity of $(\text{Be}_2\text{SiO}_4)_{\text{ss}}$ is buffered at a significant level in willemite from the genthelvite + sphalerite + petedunnite rock. Gurvich (1963) reported willemite associated with phenakite, genthelvite, gahnite, quartz, and other minerals from a mylonite zone in the USSR. Analysis of the willemite yielded 0.53 wt% BeO , equivalent to 1.5 mol% Be_2SiO_4 . Marchenko et al. (1976) reported 0.25 wt% BeO or 0.7 mol% Be_2SiO_4 in a willemite from a granite. Palache (1935) noted that Be was detected in qualitative spectroscopic analyses of Franklin willemite. Franklin willemites (and hardystonites) should be analyzed for Be and for phenakite as well as chrysoberyl (BeAl_2O_4 , olivine structure), and gugiaite ($\text{Ca}_2\text{BeSi}_2\text{O}_7$, melilite structure) should be sought in Franklin rocks that contain some Be. In the petedunnite-bearing rock, the Be_2SiO_4 content of willemite coexisting with genthelvite and sphalerite could serve as a thermometer following calibration of Reaction 1.

PHASE EQUILIBRIA

No subsolidus experiments are available that are applicable to the system $\text{CaZnSi}_2\text{O}_6$ - $\text{Ca}(\text{Mg,Mn,Fe})\text{Si}_2\text{O}_6$, so it is difficult to evaluate the stability of natural petedunnite. A few experiments available at high temperatures and pressures in simple systems and assemblages reported

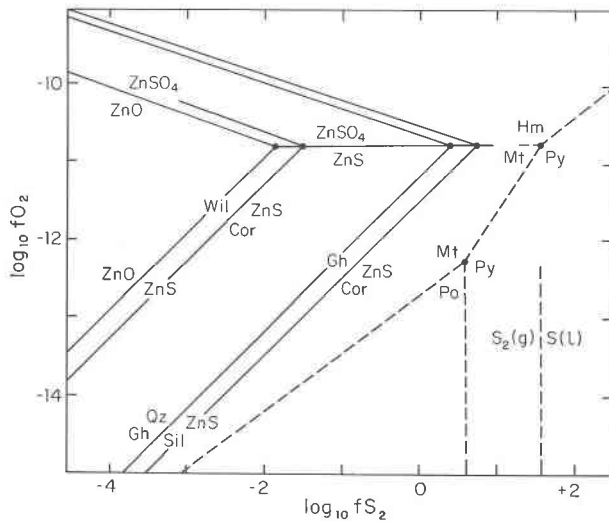


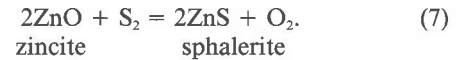
Fig. 2. Stability of phases in the system Zn-Al-Si-O-S as a function of f_{S_2}/f_{O_2} and comparison with reactions in the system Fe-O-S at 5 kbar and 1000 K. At high f_{O_2} , reactions involving ZnS are replaced with an analogous reaction with ZnSO₄ involving a slope change at the ZnS-ZnSO₄ boundary. Note the restriction of willemite (Zn₂SiO₄) and zincite (ZnO) to high f_{O_2}/f_{S_2} compared to the stability of pyrrhotite and pyrite. These reactions were calculated with the data in Table 4 and from Robie et al. (1978) for Fe-O-S phases at 5 kbar and 1000 K using $\Delta G_{1000K}^0 = 0 = \Delta G_{298}^0 + \Delta V\Delta P + RT\ln(f_{S_2}^n \cdot f_{O_2}^m)$, where n and m are stoichiometric coefficients in an equation for a given reaction and T is in kelvins. Hm = hematite, Po = pyrrhotite, Py = pyrite, Mt = magnetite; see Table 5 for other abbreviations.

represent an equilibrium assemblage. Petedunnite and hardystonite contain little Al (Palache, 1935; Louisnathan, 1969; this work), and Reactions 3 and 5 are apparently driven far to the left during the formation of these minerals at Franklin.

The system Zn-O-S

This system contains limiting reactions among zinc oxides, sulfides, and sulfates. Ingraham and Kellogg (1963) experimentally desulfidized ZnSO₄ and ZnO·2ZnSO₄ at

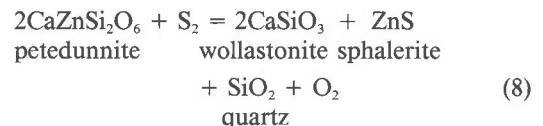
950–1200 K and calculated phase equilibria with ZnS and ZnO for variable pressures of SO₂ and O₂. We have recalculated the same equilibria with respect to S₂ and O₂ fugacities (Fig. 2). Occurrences of zincite and sphalerite at Franklin will restrict ratios of f_{O_2}/f_{S_2} by the reaction:



Schaefer (1978) has investigated this reaction electrochemically at 950 to 1200 K. Recalculation of his results at 1000 K for f_{S_2} of 10^{-5} yields $f_{O_2} = 10^{-13.3}$, in good agreement with the calculated value of $10^{-13.0}$ using the data in Table 5. These f_{O_2} values are some four orders of magnitude higher than those indicated for the stability of iron sulfides (Fig. 2). Zinc sulfates would require higher f_{O_2} than ZnO and ZnS. However, the high solubilities of the zinc sulfates suggest that they would remain dissolved under most geologic conditions.

The system Ca-Zn-Si-O-S

The reaction



will limit the solid solution of petedunnite component in clinopyroxene coexisting with wollastonite + sphalerite + quartz and should provide measurable Zn in such pyroxenes. Preliminary microprobe measurements of two skarn pyroxenes from sphalerite deposits yield 0.08 and 0.13 wt% ZnO, corresponding to 0.2 and 0.4% CaZnSi₂O₆. At lower f_{S_2} , these contents should increase, and Reaction 8 could be used to define a - X relations in pyroxene solid solutions with CaZnSi₂O₆. At higher f_{CO_2} , a pyroxene would have its CaZnSi₂O₆ content buffered by sphalerite + calcite + quartz instead. These and other reactions in P - T - f_{O_2} - f_{S_2} - f_{CO_2} space may be calculated once thermodynamic data are available for CaZnSi₂O₆.

Table 5. Molar volumes and free energies (from elements) for phases in the system Zn-Al-Si-O-S

Phase	Abbrev.	Formula	V_{298}^0 (cm ³)	Ref.	$-\Delta G_{1000}^0$ (kJ)	Ref.
Sphalerite	ZnS	ZnS	23.83	(1)	170.7	(5, 11)
Corundum	Cor	Al ₂ O ₃	25.58	(1)	1361.2	(6)
Quartz	Qz	SiO ₂	22.69	(1)	730.0	(6)
Zincite	ZnO	ZnO	14.34	(1)	246.8	(7, 11)
Gahnite	Gh	ZnAl ₂ O ₄	39.79	(2)	1646.7	(8, 11)
Zinc sulfate	ZnSO ₄	ZnSO ₄	41.57	(2)	590.9	(9, 11)
Zinc oxysulfate	Zn ₃ O(SO ₄) ₂	Zn ₃ O(SO ₄) ₂	103.59	(3)	1442.6	(9, 11)
Willemite	Wil	Zn ₂ SiO ₄	52.51	(4)	1231.1	(10, 11)
Sillimanite	Sil	Al ₂ SiO ₅	49.90	(1)	2095.0	(6)

Note: References are (1) Robie et al., 1978; (2) JCPDS, 1974; (3) Bald and Gruehn, 1981; (4) Klaska et al., 1978; (5) Mills, 1974; (6) Hemingway et al., 1982; (7) Wilder, 1969; Katayama et al., 1982; (8) Jacob, 1976; (9) Ingraham and Kellogg, 1963; (10) Kozłowska-Rog and Rog, 1979; (11) Appendix 1.

- Bald, L., and Gruehn, R. (1981) Die Kristallstruktur von einem Sulfate-reichen Oxidsulfar des Zinks. *Naturwissenschaften*, 68, 39.
- Bence, A.E., and Albee, A.L. (1968) Empirical correction factors for electron microanalysis of silicates and oxides. *Journal of Geology*, 76, 382–403.
- Benner, R.L., and Kenworthy, H. (1966a) The thermodynamic properties of the $\text{ZnO-Fe}_2\text{O}_3\text{-Fe}_3\text{O}_4$ system at elevated temperatures. I. The thermodynamic properties as related to the spinel structure. U.S. Bureau of Mines Report of Investigations, 6754, 44 p.
- (1966b) The thermodynamic properties of the $\text{ZnO-Fe}_2\text{O}_3\text{-Fe}_3\text{O}_4$ system at elevated temperatures. II. The thermodynamic properties as related to zinc concentrate roasting. U.S. Bureau of Mines Report of Investigations, 6769, 16 p.
- Bunting, E.N. (1932) Phase equilibria in the system $\text{SiO}_2\text{-ZnO-Al}_2\text{O}_3$. U.S. Bureau of Standards Journal of Research, 8, 279–287.
- Burke, E.A.J., and Kieft, C. (1972) Franklinite from Långban, Sweden. *Lithos*, 5, 69–72.
- Burton, J.C., Taylor, L.A., and Chou, I-M. (1982) The $f_{\text{O}_2}\text{-T}$ and $f_{\text{S}_2}\text{-T}$ stability relations of hedenbergite and of hedenbergite-johannsenite solid solutions. *Economic Geology*, 77, 764–783.
- Chase, M.W., Jr., Curnutt, J.H., Downey, J.R., Jr., McDonald, R.A., Syverud, A.N., and Valenzuela, E.A. (1982) JANAF thermochemical tables, 1982 Supplement. *Journal of Physical and Chemical Reference Data*, 11, 695–940.
- Chatterjee, M., and Ganguli, B. (1975) Phase relationships in the system BeO-ZnO-SiO_2 . *Neues Jahrbuch für Mineralogie Monatshefte*, 518–526.
- Doroshev, A.M., Logvinov, V.M., Olesch, M., and Nekhaev, P.Yu. (1982) Phase transformations in ZnSiO_3 and Zn_2SiO_4 at high pressures. *Fiziko-Khimicheski Issledovaniya Mineraloobrazuyushchikh Sistem*, 1982, 85–97 [not seen, extracted from Chemical Abstracts, 98, 19,083 (1983)].
- Doroshev, A.M., Olesch, M., Logvinov, V.M., and Malinovskii, I.Yu. (1983) High-pressure stability of zinc orthopyroxene ZnSiO_3 and the occurrence of a new polytype of zinc orthopyroxene as a breakdown product. *Neues Jahrbuch für Mineralogie Monatshefte*, 277–288.
- Fedorov, S.V., Burkov, V.P., Semin, E.G., Komarov, E.V., and Shevyakov, A.M. (1978) Study of the thermodynamic characteristics of formation of willemite, Zn_2SiO_4 . *Journal of Applied Chemistry (USSR)*, 51, 2496–2499.
- Fron del, C. (1972) The minerals of Franklin and Sterling Hill—A check list. Wiley, New York.
- Fron del, C., and Baum, J. L. (1974) Structure and mineralogy of the Franklin zinc-iron-manganese deposit, New Jersey. *Economic Geology*, 69, 157–180.
- Fron del, C., and Ito, J. (1966) Zincian aegirine-augite and jefersonite from Franklin, N.J. *American Mineralogist*, 51, 1406–1413.
- Fron del, C., and Klein, C. (1965) Exsolution in franklinite. *American Mineralogist*, 50, 1670–1680.
- Ghose, S., Okamura, F.P., Wan, C., and Ohashi, H. (1974) Site preference of transition metal ions in pyroxene and olivine. *EOS*, 55, 467.
- Gurvich, S.I. (1963) Discovery of beryllium-bearing willemite in the U.S.S.R. *Doklady Academy of Sciences, SSSR, Earth Science Sections*, 153, 136–138.
- Hahn, Th., and Eysel, W. (1970) Solid solubility in the system $\text{ZnSiO}_4\text{-Zn}_2\text{GeO}_4\text{-Be}_2\text{SiO}_4\text{-Be}_2\text{GeO}_4$. *Neues Jahrbuch für Mineralogie Monatshefte*, 1970, 263–276.
- Hayashi, H., Nakayama, W., Hasegawa, K., Mizukusa, S., Mizuno, M., Ogiso, S., and Torii, Y. (1965a) Phase transition under high pressure (IV). Synthesis of ZnSiO_3 pyroxene. Report of Government Industrial Research Institute, Nagoya, 14, 384–388.
- Hayashi, H., Nakayama, W., Hasegawa, K., Mizukusa, S., Noguchi, T., Ogiso, S., and Takagi, H. (1965b) Phase transition under high pressure (V). Transition of Zn_2SiO_4 . Report of Government Industrial Research Institute, Nagoya, 14, 389–393.
- Helgeson, H.C., Delany, J.M., Nesbitt, H.W., and Bird, D.K. (1978) Summary and critique of the thermodynamic properties of rock-forming minerals. *American Journal of Science*, 278-A, 229 p.
- Hemingway, B.S., Haas, J.L., Jr., and Robinson, G.R., Jr. (1982) Thermodynamic properties of selected minerals in the system $\text{Al}_2\text{O}_3\text{-CaO-SiO}_2\text{-H}_2\text{O}$ at 298.15 K and 1 bar (10^5 pascals) and at higher temperatures. U.S. Geological Survey Bulletin, 1544, 70 p.
- Hosmer, P.K., and Krikorian, O.H. (1980) The high-temperature enthalpies of zinc sulfate and zinc oxy-sulfate. *High Temperatures-High Pressures*, 12, 281–290.
- Ingraham, T.R., and Kellogg, H.H. (1963) Thermodynamic properties of zinc sulfate, zinc basic sulfate, and the system Zn-S-O . *Metallurgical Society of AIME Transactions*, 227, 1419–1426.
- Ito, E., and Matsui, Y. (1974) High-pressure synthesis of ZnSiO_3 ilmenite. *Physics of the Earth and Planetary Interiors*, 9, 344–352.
- Jacob, K.T. (1976) Gibbs free energy of ZnAl_2O_4 and ZnCr_2O_4 . *Thermochimica Acta*, 15, 79–87.
- JCPDS. (1980) Selected powder diffraction data for minerals. Joint Committee on Powder Diffraction Standards, Swarthmore, Pennsylvania.
- Kameda, K., Yoshida, Y., and Sakairi, S. (1980) Activities of molten gold-zinc and silver-zinc alloys by e.m.f. measurements using zirconia solid electrolytes. *Japan Institute of Metals Journal*, 44, 671–677.
- Katayama, I., Iseda, A., Kemori, N., and Kozuda, Z. (1982) Measurements of standard Gibbs energies of formation of ZnO and ZnGa_2O_4 by e.m.f. method. *Japan Institute of Metals Transactions*, 23, 556–562.
- Kitchener, J.A., and Ignatowicz, S. (1951) Reduction equilibria of zinc oxide and zinc silicate with hydrogen. *Faraday Society Transactions*, 47, 1278–1286.
- Klaska, K.-H., Eck, J.C., and Pohl, D. (1978) New investigation of willemite. *Acta Crystallographica*, B34, 3324–3325.
- Kozłowska-Rog, A., and Rog, G. (1979) Thermodynamics of zinc and cobalt silicates. *Polish Journal of Chemistry*, 53, 2083–2086.
- Louisnathan, S.J. (1969) Refinement of the crystal structure of hardystonite, $\text{Ca}_2\text{ZnSi}_2\text{O}_7$. *Zeitschrift für Kristallographie*, 130, 427–437.
- Marchenko, E.Ya., Metalidi, S.V., and Sizova, R.G. (1976) Formation conditions of endogenic willemite. *Dokladi Akademii Nauk Ukrainian SSR, Series B*, 974–976.
- Mason, B. (1946) A zincian vredenbergit from Franklin, New Jersey. *Geologiska Foreningens i Stockholm Forhandlingar*, 68, 51–55.
- Mills, K.C. (1974) Thermodynamic data for inorganic sulfides, selenides and tellurides. Butterworths, London.
- Morimoto, N., Nakajima, Y., Syono, Y., Akimoto, S., and Matsui, Y. (1975) Crystal structures of pyroxene type ZnSiO_3 and $\text{ZnMgSi}_2\text{O}_6$. *Acta Crystallographica*, B31, 1041–1049.
- Muan, A. (1971) The system ZnO-CoO-SiO_2 at 1 atm. *Carnegie Institution of Washington Year Book* 69, 195–198.
- Navrotsky, A. (1971) Thermodynamics of formation of the silicates and germanates of some divalent transition metals and of magnesium. *Journal of Inorganic and Nuclear Chemistry*, 33, 4035–4050.
- Navrotsky, A., and Kleppa, O.J. (1968) Thermodynamics of formation of simple spinels. *Journal of Inorganic and Nuclear Chemistry*, 30, 479–498.
- Nesbitt, B.E. (1979) Regional metamorphism of the Ducktown, Tennessee, massive sulfides and adjoining portions of the Blue Ridge province. Ph.D. thesis, University of Michigan, Ann Arbor.
- Nysten, P. (1984) A willemite-bearing petrogenesis from Lång-

- ban. Geologiska Foreningens i Stockholm Forhandlingar, 105, 273–274.
- Olesch, M., Doroshev, A.M., and Nekhaev, P.Yu. (1982) Low pressure stability of zinc clinopyroxene (ZnSiO_3). Neues Jahrbuch für Mineralogie Monatshefte, 1982, 312–320.
- Palache, C. (1935) The minerals of Franklin and Sterling Hill, Sussex County, N.J. U.S. Geological Survey Professional Paper 180, 135 p.
- Pankratz, L.V. (1982) Thermodynamic properties of elements and oxides. U.S. Bureau of Mines Bulletin 672, 509 p.
- Petersen, E.U. (1984) Metamorphism and geochemistry of the Geco massive sulfide deposit and its enclosing wall-rocks. Ph.D. thesis, University of Michigan, Ann Arbor.
- Ribbe, P.H., and Prunier, A.R., Jr. (1977) Stereochemical systematics of ordered $C2/c$ silicate pyroxenes. American Mineralogist, 62, 710–720.
- Ringwood, A.E., and Major, A. (1967) High pressure transformations in zinc germanates and silicates. Nature, 215, 1367–1368.
- Robie, R.A., and Hemingway, B.S. (1985) Low-temperature heat capacities and entropies of MnO (pyrolusite), Mn_3O_4 (hausmanite), Mn_2O_3 (bixbyite). Journal of Chemical Thermodynamics, 17, 165–181.
- Robie, R.A., Hemingway, B.S. and Fisher, J.R. (1978) Thermodynamic properties of minerals and related substances at 298.15°K and 1 bar (10^5 pascals) pressures and at higher temperatures (revised edition) U.S. Geological Survey Bulletin 1452, 456 p.
- Robie, R.A., Finch, C.B., and Hemingway, B.S. (1982) Heat capacities and entropies of Mg_2SiO_4 , Mn_2SiO_4 and Co_2SiO_4 between 5 and 380 K. American Mineralogist, 67, 470–482.
- Schaefer, S.C. (1978) Electrochemical determination of the Gibbs energy of formation of sphalerite: U.S. Bureau of Mines Report of Investigations 8301, 16 p.
- (1982) Electrochemical determination of thermodynamic properties of manganomanganic oxide and manganese sesquioxide. U.S. Bureau of Mines Report of Investigations 8704, 17 p.
- (1983) Electrochemical determination of thermodynamic properties of manganese sulfate and cadmium oxysulfate. U.S. Bureau of Mines Report of Investigations 8809, 20 p.
- Segnit, E.R. (1954) The system CaO-ZnO-SiO_2 . American Ceramic Society Journal, 37, 273–277.
- (1962) Three planes in the quaternary system $\text{CaO-ZnO-Al}_2\text{O}_3\text{-SiO}_2$. American Ceramic Society Journal, 37, 600–607.
- Segnit, E.R., and Holland, A.E. (1965) The system MgO-ZnO-SiO_2 . American Ceramic Society Journal, 48, 409–413.
- Smith, J.V. (1966) X-ray-emission microanalyses of rock-forming minerals. V. Clinopyroxenes near the diopside-hedenbergite join. Journal of Geology, 74, 463–477.
- Spry, P.G., and Scott, S.D. (1982) Zincian spinels as indicators of base metal sulfide deposits. GAC/MAC Program Abstracts, 7, 82.
- (1986) The stability of zincian spinels in sulfide systems and their potential as exploration guides for metamorphosed massive sulfide deposits. Economic Geology, 81, 1446–1463.
- Syono, Y., Akimoto, S.-I. and Matsui, Y. (1971) High pressure transformations in zinc silicates. Journal of Solid State Chemistry, 3, 369–380.
- Vogel, R.H., Evans, B.J., and Swartzendruber, L.J. (1976) Intrasite cation ordering and clustering in natural Mn-Zn ferrites. American Institute of Physics Conference Proceedings, 34, 125–127.
- West, A.R., and Glasser, F.P. (1972) Crystallization of lithium magnesium zinc silicates II. Phase equilibria and the crystallization of glasses in the system $\text{Li}_4\text{SiO}_4\text{-Mg}_2\text{SiO}_4\text{-Zn}_2\text{SiO}_4\text{-SiO}_2$. Journal of Material Science, 7, 895–908.
- Wilder, T.C. (1969) The free energy of formation of ZnO(s) for the temperature range 420 to 908°C. Metallurgical Society of AIME Transactions, 245, 1370.
- Winter, G.A., Essene, E.J., and Peacor, D.R. (1981) Carbonates and pyroxenoids from the manganese deposit near Bald Knob, North Carolina. American Mineralogist, 66, 278–289.

MANUSCRIPT RECEIVED FEBRUARY 12, 1985

MANUSCRIPT ACCEPTED SEPTEMBER 2, 1986

APPENDIX 1. THERMODYNAMIC DATA BASE FOR PHASES IN THE SYSTEM Zn-Al-Si-O-S

High-temperature thermodynamic data have not been systematically tabulated for most zinc phases in the compilations of Robie et al. (1978), Helgeson et al. (1978), and Chase et al. (1982). One of the difficulties relates to low-temperature heat-capacity data and their effects on free energy, which have not been properly evaluated. For calculations of high-temperature phase equilibria, this problem can be minimized by using free-energy data derived from emf or phase-equilibrium measurements at or near the temperatures of interest. Comments are given on individual phases below due to inconsistencies in thermodynamic properties among various sources.

Zincite, ZnO

Although the data of Robie et al. (1978) and Pankratz (1982) are in good agreement for zincite based on low- T heats of formation, the emf data of Wilder (1969) from 818 to 986 K give free energies that are 1 kJ less negative. The emf data of Kameda et al. (1980) are some 3 kJ less negative than those of Wilder, but Katayama et al. (1982) give emf data for the reduction of ZnO that are in good agreement with Wilder's (1969) data. The data of Wilder and Katayama et al. have been selected (Table 5).

Sphalerite, ZnS

The free energy of sphalerite ($\Delta G_{1000}^0 = 170.7$ kJ) is taken from the compilation of Mills (1974). It is 2.7 kJ less negative than that of Robie et al. (1978) and 0.8 kJ less negative than that of Helgeson et al. (1978). Schaefer (1978) calculated the ΔG_{1000}^0 of sphalerite as -168.2 kJ from emf data on Reaction 7 using old data for the ΔG^0 of ZnO . Use of the data of Katayama et al. (1982) for ZnO yields $\Delta G_{1000}^0 = -170.8$ kJ for Schaefer's data, close to the value of Mills.

Gahnite, ZnAl_2O_4

Jacob (1976) has determined the free energy of gahnite relative to ZnO and Al_2O_3 at 1000 to 1200 K with emf measurements. The result is 0.8 kJ more negative than that of Navrotsky and Kleppa (1968) at 973 K. The free energy of gahnite from the elements has been calculated from Jacob's data using the data of Hemingway et al. (1982) for Al_2O_3 and the data of Katayama et al. (1982) for ZnO .

Spry and Scott (1986) reported experiments and calculations on the stability of gahnite (ss) in the system Zn-Fe-Al-S-O . Although their data may be used to constrain $a\text{-X}$ relations for spinel solid solutions, no new thermodynamic data were provided for gahnite.

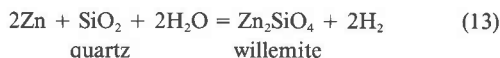
Zinc sulfates, ZnSO_4 and $\text{Zn}_3\text{O(SO}_4)_2$

Ingraham and Kellogg (1963) measured fluid pressures over decomposing zinc sulfates at $T = 950\text{--}1210$ K. Hosmer and Krikorian (1980) used Ingraham and Kellogg's data in combi-

nation with their own measured enthalpy changes to calculate the thermodynamic properties of the zinc sulfates. Unfortunately, Hosmer and Krikorian's equation for ΔG vs. T appears to generate erroneous results. However, knowledge of the free energies of SO_3 (Robie et al., 1978) and ZnO (Katayama et al., 1982) allows direct calculation of the free energies of the zinc sulfates from the data of Ingraham and Kellogg. For ZnSO_4 , the result is only 1 kJ less negative than that reported in Robie et al. (1978) based on low- T measurements. The data in Table 5 indicate that zinc oxysulfate is less stable than $\text{ZnSO}_4 + \text{ZnO}$, and thus it does not appear as a stable phase in Figure 2.

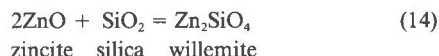
Willemite, Zn_2SiO_4

Only room-temperature data are given for willemite by Robie et al. (1978). Fedorov et al. (1978) attempted low-pressure experiments on the reaction



at $T = 773\text{--}973$ K and calculated thermodynamic parameters for willemite. Calculations using their derived free energies indicate that willemite is less stable than ZnO and SiO_2 . Fedorov et al. corrected for the partial pressure of Zn gas in Reaction 13, but this is erroneous if the experiments contained excess pure Zn liquid ($a_{\text{Zn}} = 1$) as described. Unfortunately, recalculation of the free energy of willemite from their data on $P_{\text{H}_2}/P_{\text{H}_2\text{O}}$ without P_{Zn} does not improve the results, and their pressure measurements may be inaccurate. Alternatively, willemite may simply be unreactive at these relatively low temperatures, and Fedorov et al. may have measured the activities of O-H gases in liquid Zn instead. In any case, their thermodynamic data for willemite are erroneous.

Kozłowska-Rog and Rog (1979) obtained the free energy for the reaction



using emf measurements. Their data compare well with the 298 K values in Robie et al. (1978), are within 1.8 kJ of the heat of formation measured at 965 K by Navrotsky (1971), and are nearly identical to the free energies calculated from the early reduction data of Kitchener and Ignatowicz (1951). Combining the data of Kozłowska-Rog and Rog with the free energy of ZnO and SiO_2 allows calculation of the free energy of Zn_2SiO_4 (Table 5). The remaining uncertainty is in the choice of the silica polymorph, which was not specified by Kozłowska-Rog and Rog, but was assumed by us to be quartz. If tridymite or cristobalite was involved in the experiments instead, the free energy of willemite should be reduced by 0.3 or 0.9 kJ respectively, a small correction compared to remaining uncertainties derived from the free energy of ZnO .

Muan (1971) calculated the free energy of willemite from the oxides based on the partitioning of Zn/Co between ZnO (ss) and Zn_2SiO_4 (ss) using previously determined activity coefficients for ZnO-CoO (ss). His ΔG for willemite is ~ 10 kJ more negative than those of the other workers above. Muan's experiments are apparently unreversed, and his datum has been ignored for the purposes of this paper.

Estimated errors

Realistic estimates of errors in the free energies of the above Zn phases are still considered to be plus or minus several kilojoules per mole, approximately equivalent to half a log unit error in calculated f_{O_2} or f_{S_2} . Redetermination of the free energies by emf methods in one laboratory with similar cells should reduce the relative errors. Nevertheless, the data compiled in Table 5 are considered sufficiently accurate for calculations of the phase equilibria in Figure 2.